

# Observation of the Kondo Effect in a Spin- $\frac{3}{2}$ Hole Quantum Dot

O. Klochan,<sup>1,\*</sup> A.P. Micolich,<sup>1</sup> A.R. Hamilton,<sup>1,†</sup> K. Trunov,<sup>2</sup> D. Reuter,<sup>2</sup> and A. D. Wieck<sup>2</sup>

<sup>1</sup>*School of Physics, University of New South Wales, Sydney NSW 2052, Australia.*

<sup>2</sup>*Angewandte Festkörperphysik, Ruhr-Universität Bochum, D-44780 Bochum, Germany*

(Dated: October 26, 2018)

We report the observation of Kondo physics in a spin- $\frac{3}{2}$  hole quantum dot. The dot is formed close to pinch-off in a hole quantum wire defined in an undoped AlGaAs/GaAs heterostructure. We clearly observe two distinctive hallmarks of quantum dot Kondo physics. First, the Zeeman spin-splitting of the zero-bias peak in the differential conductance is independent of gate voltage. Second, this splitting is twice as large as the splitting for the lowest one-dimensional subband. We show that the Zeeman splitting of the zero-bias peak is highly-anisotropic, and attribute this to the strong spin-orbit interaction for holes in GaAs.

PACS numbers: 72.15.Qm, 73.63.-b, 75.70.Tj

The observation of an unexpected minimum in the low temperature resistance of metals by de Haas in 1933 was ultimately explained thirty years later by Kondo as being due to interactions between a single magnetic impurity and the sea of conduction electrons in a metal [1, 2]. More recently there has been a resurgence of interest in the Kondo effect, following the discovery that the conductance of a few electron quantum dot in the Coulomb blockade regime is enhanced when the dot contains an odd number of electrons [3–5]. There is a direct analogy with the Kondo effect in metals, with the localized electron in the quantum dot acting as a magnetic impurity that interacts with the two-dimensional sea of electrons in the source and drain reservoirs.

Studies of the Kondo effect in bulk systems have progressed since the 1960s, with the focus shifting towards manifestations of Kondo physics in the strongly correlated electron systems formed in cuprates and heavy-fermion metals [6]. More precise control via improved electrostatic gate design has similarly allowed progress towards the study of more exotic manifestations of Kondo phenomena in quantum dots such as the integer-spin [7–9], two-impurity [10], and orbital Kondo effects [11]. Thus far all quantum dot Kondo studies have involved electrons, and GaAs hole quantum dots present an interesting next step. Holes in GaAs originate from  $p$ -like orbitals and behave as spin- $\frac{3}{2}$  particles due to strong spin-orbit coupling [12]. In two- and one-dimensional systems, the spin- $\frac{3}{2}$  nature of holes leads to remarkable, highly-anisotropic phenomena [13–17] not observed in electron systems, and new physics is expected for hole quantum dots also [18]. Studies of Kondo physics in hole quantum dots may also provide useful connections to recent studies in bulk strongly correlated systems [19, 20].

Here we report the observation of the Kondo effect in a GaAs hole quantum dot. Due to the poor stability of conventional gate-defined modulation doped struc-

tures [21] it has not been possible to define hole quantum dots small enough for studies of Kondo physics [4]. Instead, we follow the approach of Sfigakis *et al.* [22], where roughness in the walls of a wet-etched quantum wire led to formation of an incidental quantum dot exhibiting Kondo physics as the wire approached pinch-off. A key advantage to this approach is the ability to obtain an independent estimate of the effective Landé  $g$ -factor  $g^*$ . Using this we have fabricated a small hole quantum dot and conclusively demonstrate the “smoking gun” for Kondo physics [23] – a splitting of the zero-bias peak in the differential conductance that opens as  $2g^*\mu_B B$  in response to an in-plane magnetic field  $B$  and is independent of the gate voltage [4, 5]. In contrast to electrons, we find that the field splitting of the zero-bias peak is highly anisotropic.

We used a heterostructure consisting of the following layers grown on a (100)-oriented substrate: 1  $\mu\text{m}$  undoped GaAs, 160 nm undoped AlGaAs barrier, 10 nm undoped GaAs spacer and a 20 nm GaAs cap degenerately doped with carbon for use as a metallic gate [24, 25]. A (100) heterostructure was used to avoid the crystallographic asymmetries that plague (311)A heterostructures [16, 17]. Ohmic contacts are made with AuBe alloy annealed at 490°C for 60 s. Our devices are remarkably stable, owing to population with holes electrostatically rather than by ionized modulation dopants [24, 25]. A 300 nm long by 300 nm wide quantum wire aligned along the  $[01\bar{1}]$  crystallographic direction is fabricated by electron beam lithography, as shown in the lower left inset to Fig. 1(a). The quantum wire is defined by shallow etching the doped cap to a depth  $\sim 25$  nm to form three gates – a central top-gate negatively biased to  $V_{TG}$  to control the hole density and two side-gates positively biased to  $V_{SG}$  to control the electrostatic width of the wire [17, 25]. The quantum dot forms as the wire approaches pinch-off, as discussed in the following paragraph. All data were obtained at  $V_{TG} = -0.67$  V corresponding to a 2D hole density  $p = 2 \times 10^{11} \text{ cm}^{-2}$  and mobility  $\mu = 450,000 \text{ cm}^2/\text{Vs}$ . We used standard lock-in techniques to measure the two terminal differential conductance  $G'(V_{SD})$  with a variable dc source-drain bias  $V_{SD}$  added to a constant 15  $\mu\text{V}$

\* klochan@phys.unsw.edu.au

† Alex.Hamilton@unsw.edu.au

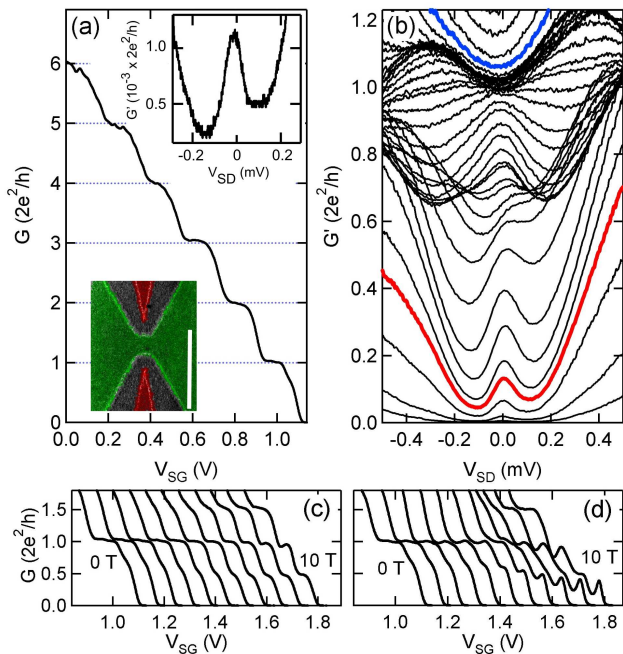


FIG. 1. (a) Linear conductance  $G$  vs side-gate voltage  $V_{SG}$  for our device, the dot forms at  $G < 2e^2/h$  (see text). Lower left inset: Scanning electron micrograph of the device with top-gate (green) and side-gates (red) separated by etched trenches (grey). The scale bar indicates  $1 \mu\text{m}$ . Upper right inset: Differential conductance  $G'$  vs dc source-drain bias  $V_{SD}$  at a side-gate voltage  $V_{SG} = 1.115 \text{ V}$  showing the zero-bias peak at  $10^{-3} \times 2e^2/h$ . (b)  $G'$  vs  $V_{SD}$  for various  $V_{SG}$  starting at  $1.1 \text{ V}$  (bottom) and stepping sequentially by  $-5 \text{ mV}$  to  $0.9 \text{ V}$  (top). The red trace ( $V_{SG} = 1.085 \text{ V}$ ,  $G < e^2/h$ ) shows enhanced conductance centered at  $V_{SD} = 0$  while the blue trace ( $V_{SG} = 0.91 \text{ V}$ ,  $G > 2e^2/h$ ) shows the standard parabolic dependence of  $G'$  on  $V_{SD}$ . (c/d)  $G$  vs  $V_{SG}$  for increasing in-plane magnetic field (c) parallel to ( $B_{\parallel}$ ) and (d) perpendicular to ( $B_{\perp}$ ) the wire. Traces obtained with a  $+1 \text{ T}$  increment and offset to the right by  $+0.07 \text{ V}$  for clarity.

ac excitation at  $5 \text{ Hz}$ . A constant series resistance of  $30.5 \text{ k}\Omega$  was subtracted from all measurements presented. The experiment was performed in a dilution refrigerator with a base temperature of  $25 \text{ mK}$ , which featured an *in-situ* rotator that enabled the sample to be reoriented with respect to the applied magnetic field  $B$  without the sample temperature exceeding  $200 \text{ mK}$  [26].

Figure 1(a) shows the linear conductance  $G = G'(V_{SD} = 0)$  versus  $V_{SG}$  with the six quantized conductance plateaus confirming ballistic transport through the device. The quantum dot forms at  $G < 2e^2/h$  due to a combination of microscopic deviations in confining potential due to etch roughness in the gates [22] and self-consistent electrostatic effects [27]. The presence of a bound-state in this system is revealed by the evolution of  $G$  versus  $V_{SG}$  with increasing in-plane magnetic field aligned parallel  $B_{\parallel}$  [Fig. 1(c)] and perpendicular  $B_{\perp}$  [Fig. 1(d)] to the wire at  $G < 2e^2/h$ . In both

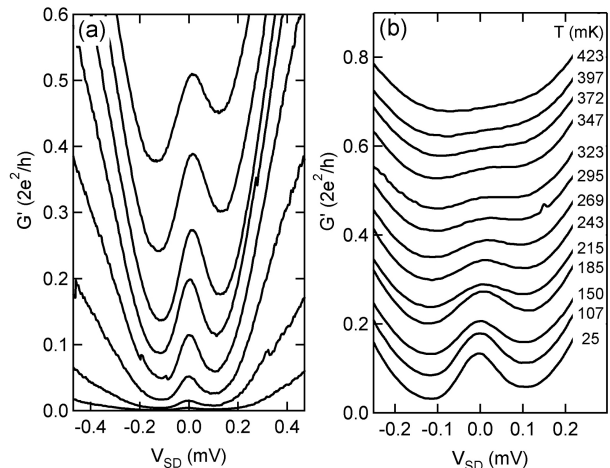


FIG. 2. (a) Asymmetric bias study of  $G'$  vs  $V_{SD}$  at various  $V_{SG}$ . Each trace directly corresponds to one in Fig. 1(b), with the two side-gate voltages set such that they differ by  $0.5 \text{ V}$  but their average equals the  $V_{SG}$  in Fig. 1(b). The lowest trace has  $V_{SG}^1 = 0.85 \text{ V}$  and  $V_{SG}^2 = 1.35 \text{ V}$ , which average to  $1.1 \text{ V}$  to match  $V_{SG}$  for the lowest trace in Fig. 1(b). Moving upwards, both side-gates are sequentially incremented by  $-5 \text{ mV}$  for each trace, the uppermost trace has an average  $V_{SG} = 1.065 \text{ V}$ . (b)  $G'$  vs  $V_{SD}$  at fixed  $V_{SG} = 1.085 \text{ V}$  for different temperatures  $T$ . Traces are sequentially offset by  $+0.05 \times 2e^2/h$  from bottom.

cases, plateaus at  $e^2/h$  and  $3e^2/h$  emerge, indicating the onset of spin-splitting [28], accompanied by sharp resonances signalling formation of a bound-state within the wire [22, 29–31]. We will show later in Fig. 2(a) that this bound-state is not an impurity effect, as it is robust to gate-induced lateral shifting of the 1D channel [32]. Coupling of the magnetic field to orbital motion [33] may be responsible for differences in resonant structure between Figs. 1(c/d), as any random disorder potential should be constant given both orientations were measured during a single cooldown.

A study of the zero-bias peak (ZBP) in the differential conductance provides additional evidence for quantum dot formation. Figure 1(b) shows  $G'$  versus  $V_{SD}$  at a range of  $V_{SG}$  spanning  $0 < G < 1.2 \times 2e^2/h$ , with two traces highlighted. Under a single particle picture,  $G'$  should depend quadratically on  $V_{SD}$  with a minimum at  $V_{SD} = 0$  [34], as observed for the blue trace at  $G > 2e^2/h$  in Fig. 1(b). In contrast at  $G < 2e^2/h$ ,  $G'$  shows a pronounced peak at  $V_{SD} = 0$  superimposed upon a parabolic background [red trace, Fig. 1(b)], known as the zero-bias peak. We observe the ZBP at conductances as low as  $10^{-3} \times 2e^2/h$ , consistent with previous work [22, 35, 36]. This is demonstrated upper right inset to Fig. 1(a).

To demonstrate that the ZBP is robust and not due to random disorder [37], we have studied the ZBP as the wire is shifted laterally. We do this by repeating each measurement in Fig. 1(b) with a voltage offset of  $0.25 \text{ V}$  added to side-gate 1 and subtracted from side-gate 2,

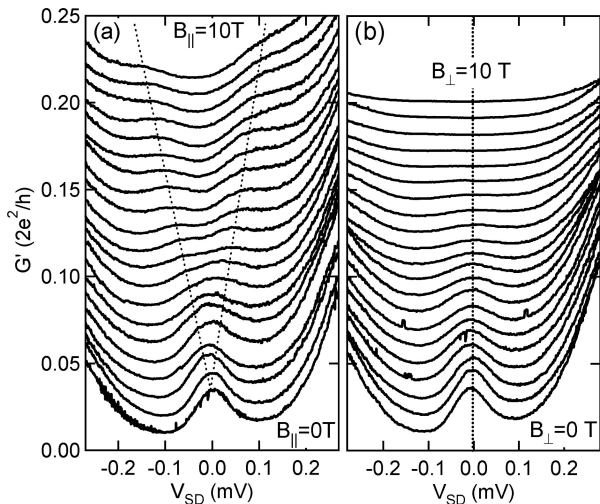


FIG. 3.  $G'$  vs  $V_{SD}$  at  $V_{SG} = 1.105$  V measured for in-plane magnetic fields ranging from 0 to 10 T oriented (a) parallel to ( $B_{\parallel}$ ) and (b) perpendicular to ( $B_{\perp}$ ) the wire. Traces obtained with a  $+0.5$  T increment and sequential vertical offset of  $+0.01 \times 2e^2/h$  from the bottom.

such that the average bias is maintained to facilitate direct comparison. This results in a lateral shift of the wire by  $\approx 60$  nm [32], and gives the data shown in Fig. 2(a). For traces below  $e^2/h$  there is almost no change in the ZBP compared to the data from the unshifted channel in Fig. 1(b), confirming that the ZBP is not disorder-induced. Equivalent data was obtained when we shifted the channel in the opposite direction (not shown). To further check the consistency of our ZBP with the known Kondo physics of electron quantum dots, in Fig. 2(b) we show the evolution of the red trace from Fig. 1(b) with temperature  $T$ . The peak widens and decreases in amplitude with increasing  $T$ , consistent with previous studies [5].

We now focus on the magnetic field dependence of the zero-bias peak looking for: a) the  $g^*$  anisotropy characteristic of spin- $\frac{3}{2}$  holes, and b) the distinctive  $2g^*\mu_B B$  peak splitting of Kondo physics. We begin by examining the evolution of the ZBP with  $B_{\parallel}$  in Fig. 3(a). Initially no splitting is resolved and the only change is a widening of the zero-bias peak. However, at  $B_{\parallel} \approx 4$  T two peaks become resolved, and these separate in  $V_{SD}$  as  $B_{\parallel}$  is increased further. The behavior is very different with an in-plane field  $B_{\perp}$  applied perpendicular to the wire [Fig. 3(b)]. Here the peak shows no splitting even at the highest field  $B_{\perp} = 10$  T; instead the peak is gradually reduced in amplitude and ultimately suppressed entirely. This anisotropic behavior matches the underlying  $g^*$  anisotropy of the 1D wire [17] in which the dot resides. We return to this anisotropy in the final discussion, and now continue with quantitative analysis of the peak splitting with  $B_{\parallel}$ .

As pointed out by Cronenwett *et al.* in Ref. [5], the most distinct sign of the quantum dot Kondo effect is a

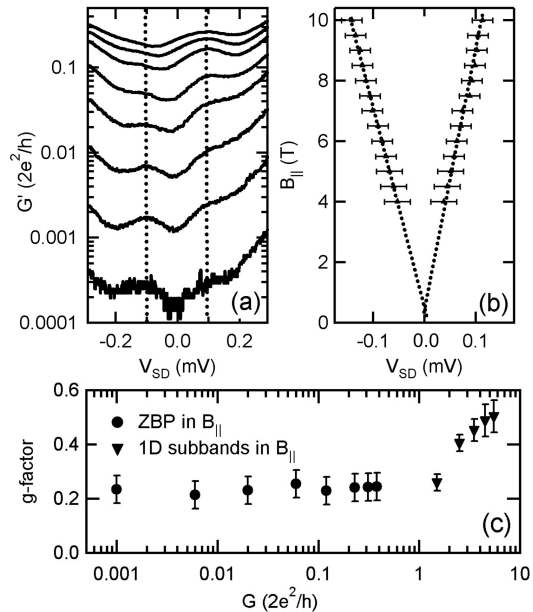


FIG. 4. (a) Plot of  $G'$  vs  $V_{SD}$  at various  $V_{SG}$  at fixed  $B_{\parallel} = 8$  T demonstrating the gate voltage independence of the splitting. (b) Location of the spin-split zero-bias peaks in  $V_{SD}$  ( $x$ -axis) vs  $B_{\parallel}$  for the data from Fig. 3(a). (c) Measured  $g$ -factor  $g^*$  for  $B_{\parallel}$  vs  $G$  for the zero-bias peak (solid circles) at  $G < 2e^2/h$  and 1D subbands (solid triangles) at  $G > 2e^2/h$ .

gate voltage independent ZBP split by  $2g^*\mu_B B$ . Figure 4(a) shows  $G'$  versus  $V_{SD}$  at various  $V_{SD}$  at  $B_{\parallel} = 8$  T. The two vertical dotted lines in Fig. 4(a) pass through the field-split zero-bias peaks over more than three orders of magnitude in conductance, demonstrating the gate voltage independence of the peak splitting. Turning to the splitting as a function of field, in Fig. 4(b) we plot the peak location in  $V_{SD}$  for the traces in Fig. 3(a) where two peaks can be clearly resolved against  $B_{\parallel}$ . The peak locations are determined by eye and the error bars are estimated knowing that the ZBP sits on a parabolic background with a slight linear asymmetry from the way that  $V_{SD}$  is applied in the measurement circuit. The ZBP clearly splits linearly with  $B_{\parallel}$  in Fig. 4(b), giving  $g_{ZBP}^* = 0.23 \pm 0.05$  if we assume a splitting  $eV_{SD} = 2g_{ZBP}^*\mu_B B$ . The data will justify this assumption below. We repeated this analysis at eight different conductances between  $10^{-3}$  and  $0.5 \times 2e^2/h$  giving the solid circles plotted in Fig. 4(c). The error bars are obtained from a regression analysis of linear fits such as that in Fig. 4(b). The  $g_{ZBP}^*$  values obtained are constant over three orders of magnitude in  $G$ , in agreement with Fig. 4(a), and give an average  $g_{ZBP}^* = 0.236 \pm 0.012$ .

A natural question is: How do we know that the peak splitting is given by  $2g^*\mu_B B$  rather than  $g^*\mu_B B$ , which would increase the  $g^*$  extracted from the data by a factor of two? The key advantage of our device is that we can use 1D subband spectroscopy [28] to independently measure  $g^*$  in the limit where  $G$  approaches

$2e^2/h$  from above. This allows us to corroborate our measurement of  $g_{\text{ZBP}}^*$ . We measure  $g_{\text{1D}}^*$  for the first five 1D subbands using the method in Ref. [17] and the usual Zeeman expression  $g_{\text{1D}}^* \mu_B B$  for 1D subbands [28]. The resulting  $g_{\text{1D}}^*$  values, plotted as solid triangles in Fig. 4(c), decrease linearly as  $G$  approaches  $2e^2/h$ . This linear decrease is distinctive of holes in (100) heterostructures [17]. However, the most significant aspect is that the  $g_{\text{1D}}^* = 0.25 \pm 0.03$  obtained for the lowest 1D subband assuming the 1D splitting goes as  $g^* \mu_B B$  is in excellent agreement with  $g_{\text{ZBP}}^*$  obtained assuming the ZBP splitting goes as  $2g^* \mu_B B$ . This is “smoking gun” evidence confirming our observation of Kondo physics in a hole quantum dot [4, 5, 23].

We conclude by discussing some key implications of our findings. The magnitude and anisotropy of  $g_{\text{ZBP}}^*$  closely matches that of  $g_{\text{1D}}^*$  for the lowest 1D subband. This suggests that  $g_{\text{ZBP}}^*$  is set by the prevailing  $g^*$  of the environment hosting the dot. It agrees with quantum dots [5], where the splitting of the ZBP gives the same  $g^*$  as bulk GaAs, and with carbon nanotubes [38]. The fact that a spin- $\frac{3}{2}$  system produces no radical change in the observed Kondo physics is interesting, as it implies that the process only relies on the presence of a doubly-degenerate quantum dot level to mediate transport between the reservoirs, and not its precise nature/spin. This is in accordance with recent studies of more exotic manifestations of Kondo physics in quantum dots [7–11]. However, a spin- $\frac{3}{2}$  system may ultimately present more subtle changes, for example, confinement-induced

mixing [39] between heavy-hole and light-hole subbands (i.e., states with total angular momentum quantum numbers  $m_j = \pm \frac{3}{2}$  and  $\pm \frac{1}{2}$  respectively) may alter the relevant scales in the problem. Further studies in this direction would be useful, including both theoretical work and measurements from improved device geometries. Finally, we comment briefly on the bearing of our results on studies of the 0.7 anomaly [40] in 1D systems. Although we observe a plateau-like feature near  $0.7 \times 2e^2/h$  in our device (see Figs. 1(a,c,d)), the presence of the resonant structure in the linear conductance precludes any direct and definitive link between the 0.7 anomaly and the behavior we observe for our zero-bias peak. We emphasize that the gate-voltage independent Zeeman splitting of our ZBP points conclusively to the quantum dot Kondo effect, in contrast with the gate-voltage dependent zero-bias anomaly (ZBA) splitting observed in undoped quantum wires by Sarkozy *et al.* [35]. The characteristics of our zero-bias peak are very different to those of the ZBA in quantum wires. The two effects clearly have a different origin, which agrees with the suggestion by Sarkozy *et al.* [35] that the ZBA is a fundamental property of quantum wires, and suggests that it may involve processes beyond Kondo physics alone.

This work was funded by the Australian Research Council (Grant Nos. DP0772946, DP0986730, FT0990285). We thank U. Zülicke for helpful discussions, L.A. Yeoh and A. Srinivasan for development of the low temperature rotator, and J. Cochrane for technical support.

- 
- [1] W.J. de Haas, J. de Boer, and G.J. van den Berg, *Physica* **1**, 1115 (1933).
- [2] J. Kondo, *Prog. Theor. Phys.* **32**, 37 (1964).
- [3] L.P. Kouwenhoven and L.I. Glazman, *Physics World* **14**(1), 33 (2001).
- [4] D. Goldhaber-Gordon *et al.*, *Nature* **391**, 156 (1998).
- [5] S.M. Cronenwett, T.H. Oosterkamp and L.P. Kouwenhoven, *Science* **281**, 540 (1998).
- [6] G.R. Stewart, *Rev. Mod. Phys.* **73**, 797 (2001).
- [7] S. Sasaki *et al.*, *Nature* **405**, 764 (2000).
- [8] W.G. van der Wiel *et al.*, *Phys. Rev. Lett.* **88**, 126803 (2002).
- [9] G. Granger *et al.*, *Phys. Rev. B* **72**, 165309 (2005).
- [10] H. Jeong, A.M. Chang and M.R. Melloch, *Science* **293**, 2221 (2001).
- [11] P. Jarillo-Herrero *et al.*, *Nature* **434**, 484 (2005).
- [12] R. Winkler *et al.*, *Phys. Rev. Lett.* **85**, 4574 (2000).
- [13] S.J. Papadakis *et al.*, *Phys. Rev. Lett.* **84**, 5592 (2000).
- [14] R. Danneau *et al.*, *Phys. Rev. Lett.* **97**, 026403 (2006).
- [15] L.P. Rokhinson, L.N. Pfeiffer, and K.W. West, *Phys. Rev. Lett.* **96**, 156602 (2006).
- [16] O. Klochan *et al.*, *New J. Phys.* **11**, 043018 (2009).
- [17] J.C.H. Chen *et al.*, *New J. Phys.* **12**, 033043 (2010).
- [18] T. Andlauer and P. Vogl, *Phys. Rev. B* **79**, 045307 (2009).
- [19] K. Suzuki *et al.*, *Phys. Rev. B* **82**, 054519 (2010).
- [20] A. Ślebarski *et al.*, *Phys. Rev. B* **82**, 235106 (2010).
- [21] K. Ensslin, *Nat. Phys.* **2**, 587 (2006).
- [22] F. Sfigakis *et al.*, *Phys. Rev. Lett.* **100**, 026807 (2008).
- [23] Y. Meir, N.S. Wingreen, and P.A. Lee, *Phys. Rev. Lett.* **70**, 2601 (1993).
- [24] W.R. Clarke *et al.*, *J. Appl. Phys.* **99**, 023707 (2006).
- [25] O. Klochan *et al.*, *Appl. Phys. Lett.* **89**, 092105 (2006).
- [26] L.A. Yeoh *et al.*, *Rev. Sci. Instrum.* **81**, 113905 (2010).
- [27] Y. Yoon *et al.*, *Phys. Rev. Lett.* **99**, 136805 (2007).
- [28] N.K. Patel *et al.*, *Phys. Rev. B* **44**, 13549 (1991).
- [29] P.L. McEuen *et al.*, *Surf. Sci.* **229**, 312 (1990).
- [30] C.-T. Liang *et al.*, *Phys. Rev. Lett.* **81**, 3507 (1998).
- [31] Y. Komijani *et al.*, *Europhys. Lett.* **91**, 67010 (2010).
- [32] L.I. Glazman and I.A. Larkin, *Semicond. Sci. Technol.* **6**, 32 (1991).
- [33] C.H.L. Quay *et al.*, *Nature Physics* **6**, 336 (2010).
- [34] L. Martín-Moreno *et al.*, *J. Phys.: Condens. Matter* **4**, 1323 (1992).
- [35] S. Sarkozy *et al.*, *Phys. Rev. B* **79**, 161307 (2009).
- [36] Y. Ren *et al.*, *Phys. Rev. B* **82**, 045313 (2010).
- [37] T.-M. Chen *et al.*, *Phys. Rev. B* **79**, 153303 (2009).
- [38] J. Nygård *et al.*, *Nature* **408**, 343 (2000).
- [39] U. Zülicke, *Phys. Stat. Sol. (c)* **3**, 4354 (2006).
- [40] K.J. Thomas *et al.*, *Phys. Rev. Lett.* **77**, 135 (1996).